Fracture Mechanics Based Coated Particle Fuel Failure Models

Jing Wang[a], Ronald G. Ballinger[a]
([a]MIT Nuclear Engineering Department, 185 Albany Street, Cambridge, MA, 02139, USA)

ABSTRACT

The most modern gas reactor coated particle fuel design consists of a kernel of fuel, either UO_2, UCO, or PuO_2, surrounded by a low density pyrocarbon "buffer" layer, and a three-layer structure consisting of an inner dense pyrocarbon (IPyC), a SiC, and an outer dense pyrocarbon (OPyC) layer. The integrity of this layer is the key to the overall reliability of the fuel. During operation the effect of fuel fission and irradiation damage is to cause internal pressurization of the fuel as well as and increase in tensile stresses in the pyrocarbon layers. Eventual cracking of the pyrocarbon layers can cause stress concentration at the interface between the pyrocarbon and SiC layers. A fracture mechanics based model has been developed to allow analysis of fuel failure due to SiC cracking induced by pyrocarbon layer cracking. The physics of the model includes: (1) an accounting for the relaxation of stress in the pyrocarbon layers after cracking, (2) following the evolution of the stress in the pyrocarbon layer and the induced stress intensity factor in the SiC after initial PyC cracking but no SiC failure, and (2) an accurate crack tip stress intensity calculation.

1.0 INTRODUCTION

The most modern gas reactor coated particle fuel design consists of a kernel of fuel, either UO_2, UCO, or PuO_2, surrounded by a low density pyrocarbon "buffer" layer, and a three-layer structure consisting of an inner dense pyrocarbon, a SiC, and an outer dense pyrocarbon layer. Figures 1 and 2 show a schematic of and an actual coated particle of this type with typical dimensions indicated.

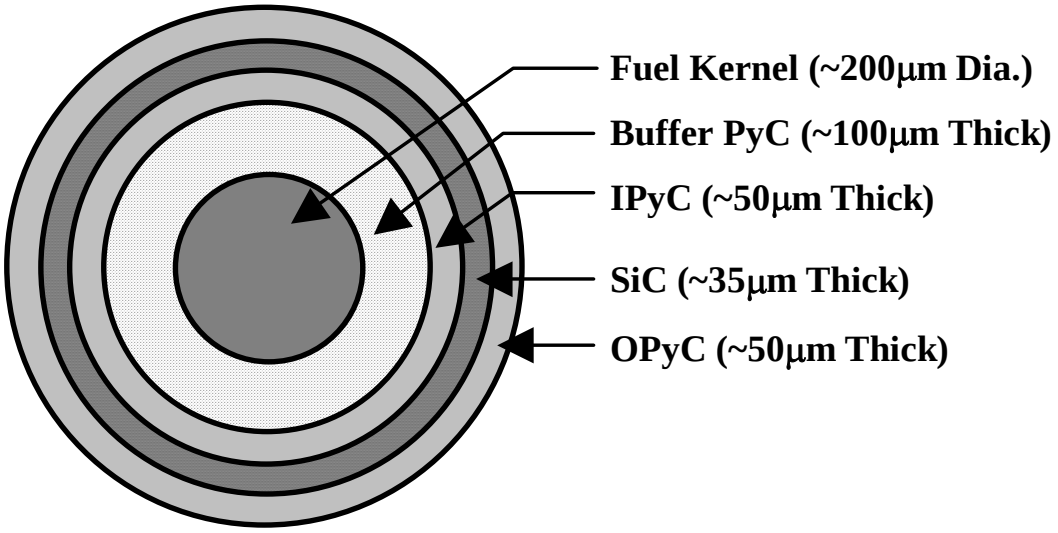

FIGURE 1. Coated particle fuel schematic.

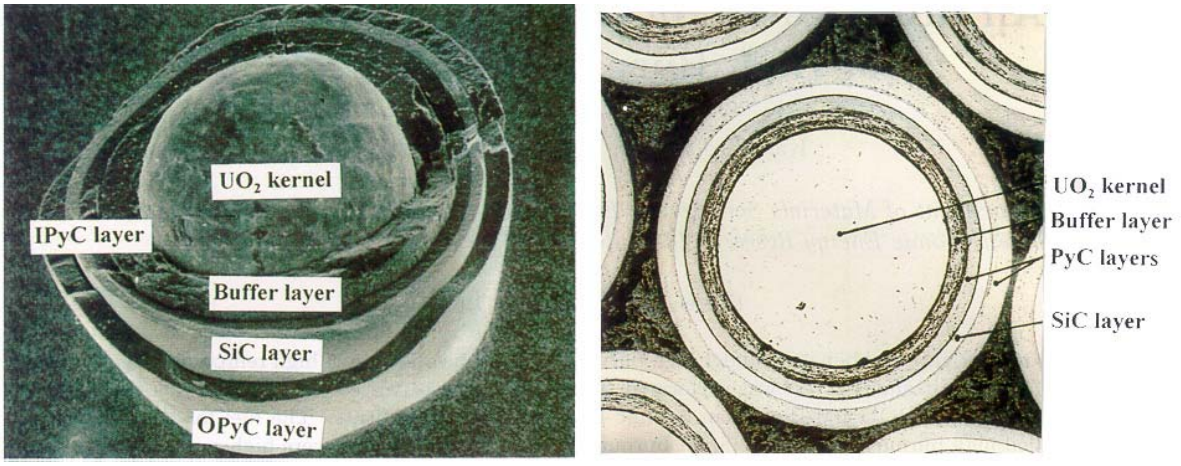

FIGURE 2. Coated particle fuel showing detailed features [1]

The buffer layer is of low density and is designed to accommodate swelling and other changes that may occur during operation. The low density also allows for the accommodation of fission gas that is released during operation. Radiation exposure results in significant densification of the buffer. The three layer system, IPyC-SiC-OPyC, form the primary barriers to fission product release with the SiC layer establishing the main pressure boundary for the particle. During operation the fission process results in the release of fission products to the buffer region. At the same time the PyC layers will tend to shrink, putting these layers in circumferential tension and the SiC layer into compression. Eventually both the OPyC and IPyC layers will develop radial cracks and/or circumferential cracks or separations at the PyC/SiC interface. As a result of these processes there will be a slow buildup of internal gas pressure within the particle that is contained by the usually intact SiC layer. The gas pressure will result from noble fission gas release as well as carbon-containing (CO/CO_2) in some cases. Additionally, other fission products, some of which are aggressive to the SiC, are also released. These include noble metals such as silver, platinum and palladium, and alkali metals such as cesium. If these elements, in particular palladium, become available in sufficient quantities, chemical attack of the SiC layer will occur. The attack can result in wastage of the SiC to the point where the integrity of the layer is destroyed.

The integrity of the coated particle during irradiation is key to the successful deployment of high temperature gas reactor technology if it is to play a role as part of any revival of the nuclear option. However, in the past, the assurance of this integrity has been far from certain. Failures have occured due to: (1) overpressure, (2) wastage of the SiC layer, (3) cracking of the PyC-SiC-PyC layer system, (4) the so-called amoeba effect at very high temperatures, and (5) any number of fabrication related defects. Figure 3 shows a micrograph of a failed particle in which the PyC-SiC-PyC layer system has been breached due to cracking. Failure due to radial cracking of the SiC layer would seem to be counterintuitive since the shrinkage of the PyC layers will assure that, absent internal pressure buildup which will only become significant at very high burnup, the SiC layer will normally be in compression. However, while the SiC layer will be maintained in general compression, the cracking of the PyC layers can, it is postulated, introduce a situation where a locally high stress intensification can be developed which results in tensile stresses at the tip of the PyC crack at the interface with the SiC layer. If this intensification is, or becomes, high enough then failure can occur by local crack initiation. In this paper we report on the development of a model for this scenario.

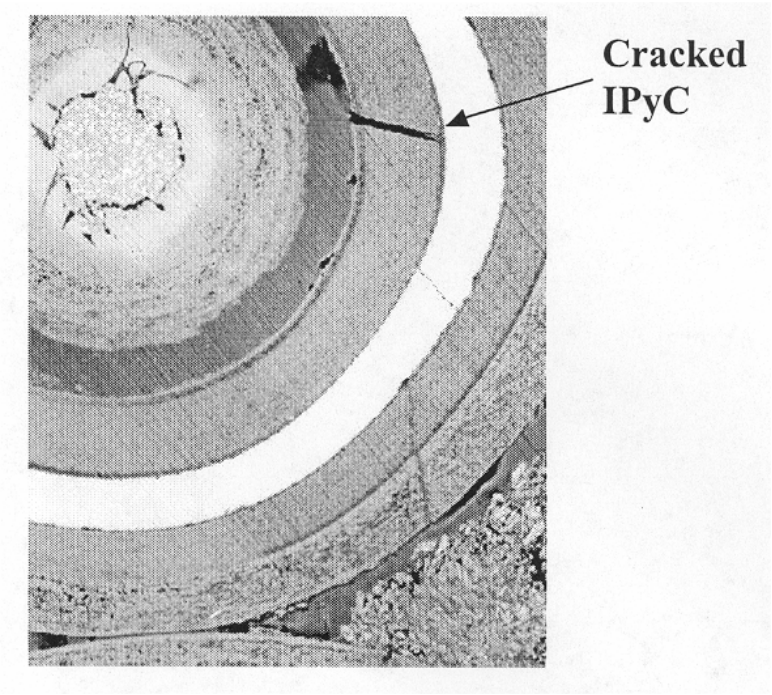

FIGURE 3. Micrograph of failed coated particle showing cracking of PyC and SiC layers [2].

Superior, and predictable, coated particle fuel performance will be essential for the development and deployment of gas cooled reactor systems for future power generation. Unfortunately, unlike light water reactor (LWR) type fuel, which can undergo 100% inspection of all individual components as well as the finished element, coated particle fuel cannot be inspected in detail other than to identify clearly failed particles, those which do not meet overall dimensional specifications or contain no fuel. For this reason, the modeling of both the fabrication process and the in-reactor performance will play a critical role in the establishment of the safety case for this type of fuel. The achievement of high reliability will require a significant development effort in a number of areas including: (1) coated particle fuel process development and manufacture, (2) in-pile testing, and (3) modeling of the overall system. Fuel performance modeling can serve as a means to develop better understanding of irradiation testing, point to improved process development, and reduce the overall development cost through a reduction in required expensive irradiation testing. However, the behavior of the coated particle fuel system is a function of many variables, several of which are not easily measurable. One of the roles of fuel modeling can be to help bridge the gap between what can be measured and what cannot. To this end new models are being developed, among which is a model, TIMCOAT, being developed at MIT [3-6] A detailed description of the initial version of the model has been reported elsewhere [3]. Figure 4 shows the results of a comparison of the model predictions vs. actual behavior of the NPR1 fuel irradiation program for an early, simplified, version of the model. The overall behavior of Kr^{85} R/B and the total failure fraction compare favorably. However, while the comparison is very favorable and represents an improvement in the ability to model coated particle fuel performance, the timing of the initial increase in R/B is under-predicted. Also, the rise to the final failure fraction is more abrupt than in the actual case. There was thus considerable room for improvement. A key factor in the success of the model thus far is the incorporation of a fracture mechanics based failure model in addition to the more common over pressure based model. Modern fuels are fabricated with enough free volume in the buffer region to preclude over pressure failure except at very high burnups. The fracture mechanics model present in the simplified version of the overall model, while capturing some of the essential physics, was in need of improvement. Although the model took into account the local stress concentration from pyrocarbon cracks, it was over

simplified in the following ways. Firstly, it treated the composite coating layers as one material and ignored the elastic mismatch between the pyrocarbon and silicon carbide layers. This simplification omits the complexity of the system when a crack encounters a bi-material interface. Secondly, the initial model did not allow for immediate stress relaxation of the system upon pyrocarbon layer cracking nor did it allow for further buildup of stresses after initial pyrocarbon cracking due to continuing radiation damage. SiC layer failure was assumed to occur coincidently with cracking of PyC layer if sufficient instantaneous tensile stress could be developed in the SiC layer. If the SiC layer did not fracture when either of the PyC layers cracked, further stress development in that particle was not considered. The effect of this restriction was to eliminate later failures of particles with previously cracked pyrocarbon layers. In this paper, we report on improvements to the initial fuel failure model to capture more of the physics of the failure process.

2.0 IMPROVED FUEL FAILURE MODEL

The physics of the model has been improved in three areas: (1) an accounting for the relaxation of stress in various layers after the pyrocarbon cracking, (2) a following of the evolution of the stress in the pyrocarbon layer and the induced stress intensity factor in the SiC after initial PyC cracking but no SiC failure, and (3) an improved crack tip stress intensity calculation. A more realistic pyrocarbon stress analysis is achieved through the use of superposition of partial solutions assuming elastic behavior. When the fracture stress of a pyrocarbon layer is reached the "relaxed" stress is calculated as follows: (1) the pyrocarbon layer is allowed to elastically contract circumferentially as if it could freely slide on the interface with the SiC layer, then (2) the resulting crack tip is closed and the amount of force necessary to do this is assumed to come from interfacial shear stress. The tensile hoop stress induced in the PyC layer is then used in the new crack tip stress intensity calculation. Future improvements in the model will account for local delamination of the layers in response to the interfacial shear stress as well as chemically induced crack initiation sites. As another improvement in the model now follows the continued evolution of the crack tip stress intensity for particles that have initially cracked but for which the resulting stress intensity is not sufficient to induce SiC failure.

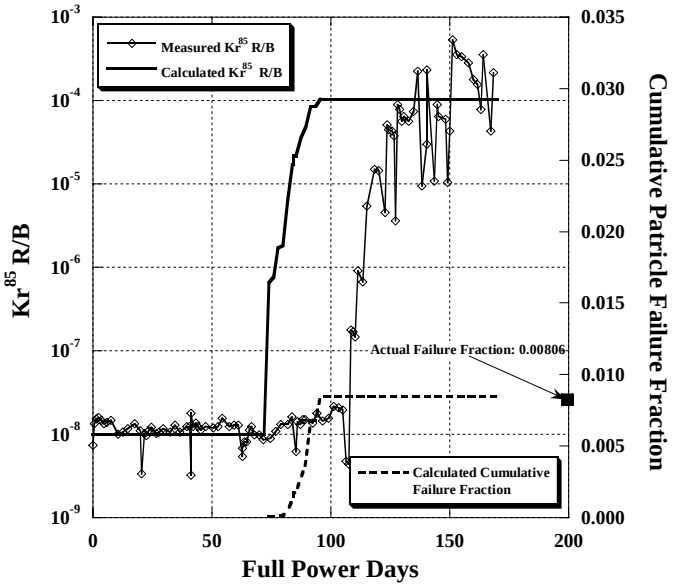

FIGURE 4 Comparison between calculated and actual R/B and failure fraction for NPR1 irradiations.

2.1 POST CRACKING STRESSES AND STRAINS

Considering the above, the following improvements are implemented in the fuel failure model. Here we use the IPyC as the cracked PyC layer as an example, as shown in Figure 5. The treatment for the OPyC layer is similar.

Firstly we look at crack configuration C in Figure 2. Based on fracture mechanics, it is well known that the displacement field around a crack tip is proportional to the square root of the distance to the crack tip, and for this analysis we assume it is approximately correct in layered materials. Using polar coordinates (r', θ') referenced to the crack tip, as shown in Figure 2, we can write the displacements as follows [9]

$$u_{r'}\left(r',\theta'\right)=\frac{K_I}{G}\sqrt{\frac{r'}{2\pi}}\cos\frac{\theta'}{2}\left(\beta-\cos^2\frac{\theta'}{2}\right), \tag{1}$$

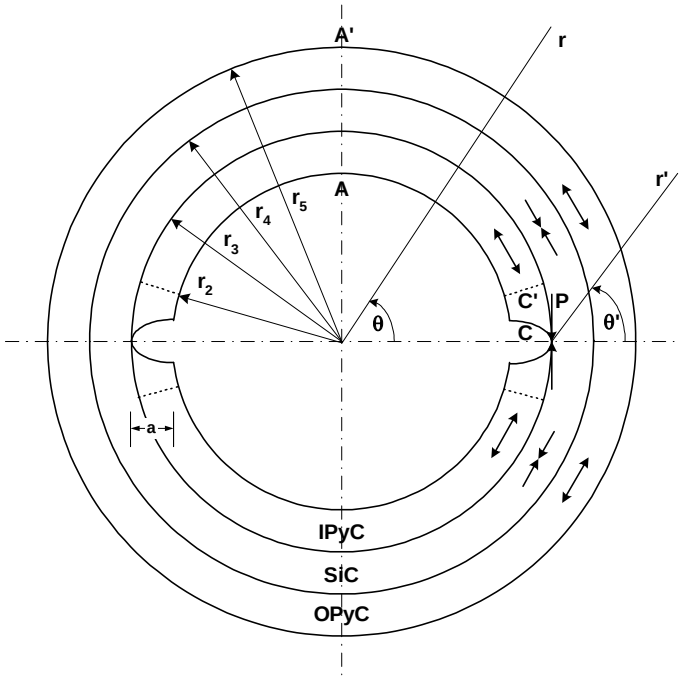

FIGURE 5. An IPyC cracked fuel particle

$$u_{\theta'}\left(r',\theta'\right)=-\frac{K_I}{G}\sqrt{\frac{r'}{2\pi}}\sin\frac{\theta'}{2}\left(\beta-\cos^2\frac{\theta'}{2}\right), \tag{2}$$

$$\beta=\begin{cases}2(1-\nu) & \text{plane strain}\\ 2\dfrac{1}{1+\nu} & \text{plane stress}\end{cases}, \tag{3}$$

where K_I is the Mode I stress intensity factor, G is shear modulus, and ν is Poisson's ratio.

It is believed that once a brittle PyC layer cracks, nothing stops the crack from propagating in the circumferential direction to form a crack ring as illustrated in Figure 2. Since the crack is axi-

symmetric, we can use the plain strain value of β [7]. Along the crack surface, θ' = π, then according to equations (1) and (2), the displacements that describe the crack configuration C are

$$u_{r'}^{C}\left(r',\pi\right)=0,\ (0\le \mathrm{r'}\le \mathrm{a}) \tag{4}$$

$$u_{\theta'}^{C}\left(r',\pi\right)=-\frac{2(1-\nu)K_I}{G}\sqrt{\frac{r'}{2\pi}},\ (0\le \mathrm{r'}\le \mathrm{a}) \tag{5}$$

or in terms of coordinates (r, θ),

$$u_{r}^{C}\left(r,0\right)=0,\ (\mathrm{r}_2\le \mathrm{r}\le \mathrm{r}_3) \tag{6}$$

$$u_{\theta}^{C}\left(r,0\right)=\frac{2(1-\nu)K_I}{G}\sqrt{\frac{r_3-r}{2\pi}},\ (\mathrm{r}_2\le \mathrm{r}\le \mathrm{r}_3). \tag{7}$$

Assume that

$$u_{\theta}^{C}\left(r,\theta\right)=u_{\theta}^{C}\left(r,0\right)\frac{\pi/2-\theta}{\pi/2}, \text{ then} \tag{8}$$

$$u_{\theta}^{C}\left(r,\theta\right)=\frac{2(1-\nu)K_I}{G\cdot\pi/2}\sqrt{\frac{r_3-r}{2\pi}}\left(\frac{\pi}{2}-\theta\right). \tag{9}$$

Our purpose is to follow stresses after the IPyC cracks. To do this, first suppose there is no resistance to free sliding of the cracked PyC layer along the interface between the SiC layer, and that the cracked PyC layer fully relaxes tangentially and reaches configuration C' in Figure 2. Then the SiC layer "applies" a shear force P to the cracked PyC layer to close the crack tip. The configuration then coincides with C with the assumption of elastic deformation. If the cracked IPyC layer, which is still subject to internal gas pressure p_i, undergoes elastic relaxation to C', the strains are

$$\varepsilon_{rr}^{C'}\left(r\right)=\frac{-\left(\sigma_{rr}\left(r\right)+p_i\right)}{E}-\frac{-\nu\sigma_{\theta\theta}\left(r\right)}{E}, \text{ and} \tag{10}$$

$$\varepsilon_{\theta\theta}^{C'}\left(r\right)=\frac{-\sigma_{\theta\theta}\left(r\right)}{E}-\frac{-\nu\left(\sigma_{rr}\left(r\right)+p_i\right)}{E}, \tag{11}$$

where $\sigma_{rr}\left(r\right)$ and $\sigma_{\theta\theta}\left(r\right)$ are stresses just before cracking, which are known from our stress analysis on intact particles [3]. According to the strain-displacement relations,

$$\varepsilon_{rr}=\frac{\partial u_r}{\partial r}, \text{ and} \tag{12}$$

$$\varepsilon_{\theta\theta}=\frac{1}{r}\frac{\partial u_\theta}{\partial\theta}+\frac{u_r}{r}, \tag{13}$$

and assuming

$$u_{r}^{C'}\left(r_3\right)=0, \text{ and} \tag{14}$$

$$u_\theta^{C'}\left(r,\frac{\pi}{2}\right)=0 \text{ due to symmetry,} \tag{15}$$

we have

$$u_r^{C'}(r_3)-u_r^{C'}(r)=\int_r^{r_3}\varepsilon_{rr}^{C'}(r)dr \text{ , so} \tag{16}$$

$$u_r^{C'}(r)=-\int_r^{r_3}\varepsilon_{rr}^{C'}(r)dr\,, \tag{17}$$

which is independent of θ, and

$$\varepsilon_{\theta\theta}^{C'}(r)=\frac{1}{r}\frac{u_\theta^{C'}\left(r,\frac{\pi}{2}\right)-u_\theta^{C'}(r,0)}{\pi/2}+\frac{u_r^{C'}(r)}{r}\text{, so} \tag{18}$$

$$u_\theta^{C'}(r,0)=\frac{\pi}{2}u_r^{C'}(r)-\frac{\pi}{2}\varepsilon_{\theta\theta}^{C'}(r)\cdot r\,. \tag{19}$$

Now assume

$$u_\theta^{C'}(r,\theta)=u_\theta^{C'}(r,0)\frac{\pi/2-\theta}{\pi/2}\text{, then} \tag{20}$$

$$u_\theta^{C'}(r,\theta)=\left[u_r^{C'}(r)-\varepsilon_{\theta\theta}^{C'}(r)\cdot r\right]\left(\frac{\pi}{2}-\theta\right). \tag{21}$$

Suppose the interfacial shear force, P, brings the cracked IPyC layer from C' back to configuration C and causes tangential stress in the IPyC layer. Then the displacement due to P is

$$u_\theta^{P}(r,\theta)=u_\theta^{C}(r,\theta)-u_\theta^{C'}(r,\theta), \tag{22}$$

and according to equations (9) and (21),

$$u_\theta^{P}(r,\theta)=\left[\frac{2(1-\nu)K_I}{G\cdot\pi/2}\sqrt{\frac{r_3-r}{2\pi}}+\varepsilon_{\theta\theta}^{C'}(r)\cdot r-u_r^{C'}(r)\right]\left(\frac{\pi}{2}-\theta\right) \tag{23}$$

Because P doesn't induce a radial stress, i.e.,

$$\sigma_{rr}^{P}=0\,, \tag{24}$$

the constitutive laws are then

$$\varepsilon_{rr}^{P}=-\frac{\nu}{E}\sigma_{\theta\theta}^{P}\text{, and} \tag{25}$$

$$\varepsilon_{\theta\theta}^{P} = \frac{1}{E}\sigma_{\theta\theta}^{P}. \tag{26}$$

From equations (25) and (26), we get

$$\varepsilon_{rr}^{P} = -\nu\varepsilon_{\theta\theta}^{P}. \tag{27}$$

From equations (12) and (27), we get

$$u_r^P(r,\theta) = -\int_r^{r_3} \varepsilon_{rr}^{P}(r,\theta)dr = \nu\int_r^{r_3} \varepsilon_{\theta\theta}^{P}(r,\theta)dr. \tag{28}$$

From equations (13) and (23), we get

$$\varepsilon_{\theta\theta}^{P}(r,\theta) = \frac{1}{r}u_r^{C'}(r) - \varepsilon_{\theta\theta}^{C'}(r) - \frac{2(1-\nu)K_I}{G\cdot\pi/2}\sqrt{\frac{r_3-r}{2\pi r^2}} + \frac{1}{r}u_r^{P}(r,\theta), \tag{29}$$

and inserting equation (28) into equation (29),

$$\varepsilon_{\theta\theta}^{P}(r,\theta) - \frac{\nu}{r}\int_r^{r_3} \varepsilon_{\theta\theta}^{P}(r,\theta)dr = \frac{1}{r}u_r^{C'}(r) - \varepsilon_{\theta\theta}^{C'}(r) - \frac{2(1-\nu)K_I}{G\cdot\pi/2}\sqrt{\frac{r_3-r}{2\pi r^2}}. \tag{30}$$

We see from equation (30) that $\varepsilon_{\theta\theta}^{P}$ is independent of θ, which is the result of assumptions in equations (8) and (20). $\sigma_{\theta\theta}^{P}$ is linked to $\varepsilon_{\theta\theta}^{P}$ by equation (26), so that after-crack stress $\sigma_{\theta\theta}^{P}$ can be calculated.

After a crack is formed in the IPyC layer, it is still subject to deformation caused by irradiation-induced dimensional change (swelling) and irradiation-induced creep. We can treat this issue as if the fully relaxed configuration C' is a function of fluence after cracking. Specifically, suppose $t-\Delta t$ is any time after cracking in the IPyC layer, then

$$\varepsilon_{rr}^{C'}(r,t) = \varepsilon_{rr}^{C'}(r,t-\Delta t) + \dot{S}_r(t-\Delta t)\Delta t, \tag{31}$$

$$\varepsilon_{\theta\theta}^{C'}(r,t) = \varepsilon_{\theta\theta}^{C'}(r,t-\Delta t) + c\sigma_{\theta\theta}^{P}(r,t-\Delta t)\Delta t + \dot{S}_t(t-\Delta t)\Delta t$$
$$= \varepsilon_{\theta\theta}^{C'}(r,t-\Delta t) + cE\varepsilon_{\theta\theta}^{P}(r,t-\Delta t)\Delta t + \dot{S}_t(t-\Delta t)\Delta t \tag{32}$$

$$u_r^{C'}(r,t) = -\int_r^{r_3} \varepsilon_{rr}^{C'}(r,t)dr, \tag{33}$$

where c is the irradiation-induced creep coefficient ($cm^2/10^{21}$neutron/MPa), and $\dot{S}_r$ and $\dot{S}_t$ are the irradiation-induced dimensional change rates ($cm^2/10^{21}$neutron) in the radial and tangential directions, respectively. The reason there is no creep term in equation (31) is that the cracked IPyC layer

transmits internal pressure to the SiC layer, and only experiences very small radial stress. Therefore the radial creep strain contribution in equation (31) is omitted. With equations (31) through (33) and equationn. (30), we then have the time dependent $\varepsilon_{\theta\theta}^{P}$, which is

$$\varepsilon_{\theta\theta}^{P}(r,t)-\frac{\nu}{r}\int_{r}^{r_3}\varepsilon_{\theta\theta}^{P}(r,t)dr = \frac{1}{r}u_r^{C'}(r,t)-\varepsilon_{\theta\theta}^{C'}(r,t)-\frac{2(1-\nu)K_I(t)}{G\cdot\pi/2}\sqrt{\frac{r_3-r}{2\pi r^2}}. \tag{34}$$

2.2 STRESS INTENSITY FACTORS

The improved stress intensity calculation makes use of a more appropriate stress intensity correlation. When a radial crack is initiated by tensile stress in either of the pyrocarbon layers, inner (IPyC) or outer (OPyC), it grows toward the PyC/SiC interface. In this case, where a crack propagates from a soft material (PyC) to a hard material (SiC), the driving force for crack growth increases first and then drops to zero as the crack reaches the interface [8]. The crack cannot grow into the SiC layer unless it is re-nucleated there. However, we know that the interface is not "smooth" due to the nature of CVD process, and that the rough inner surface of the SiC layer can provide sites for crack re-nucleation. The combination of a crack in a PyC layer and a stress riser in the SiC results in an increase in the driving force for crack re-nucleation, growth and failure of the SiC layer. It can also be seen from Reference [8] that if the crack propagates from a hard material (SiC) to a soft material (PyC), the driving force climbs quickly and the cracking is catastrophic. Thus, one would expect to see failed PyC layers without SiC cracking but not the reverse-SiC cracking but no associated PyC crack. In our model we assume that the failure of the SiC layer is tantamount to the failure of whole particle.

The resultant Mode I stress intensity factor in a radially cracked IPyC layer is given by [9]

$$K_I^{IPyC} = 0.413\frac{1+r_2/r_3}{\sqrt{1-a_{IPyC}/(r_3-r_2)}}\overline{\sigma}_{\theta\theta}^{P}(r)\sqrt{\pi a_{IPyC}}\,.. \tag{35}$$

where $\overline{\sigma}_{\theta\theta}^{P}(r)$ is the average circumferential stress in the cracked PyC layer, and we choose the crack length 'a' to be

$$a_{IPyC} = 0.99(r_3-r_2), \tag{36}$$

because strain energy release rate decreases rapidly at this level [8].

If the radial crack is in the OPyC layer, then the Mode I stress intensity factor is given by[8]

$$K_I^{OPyC} = 0.413\frac{1+r_5/r_4}{\sqrt{1-a_{OPyC}/(r_5-r_4)}}\overline{\sigma}_{\theta\theta}^{P}(r)\sqrt{\pi a_{OPyC}}\,, \tag{37}$$

Notice that equations (34) and (35) are mutually dependent, so we need iterations to find equilibrium solutions for $\sigma_{\theta\theta}^{P}$ and K_I.

We assume that the PyC crack intersects a SiC surface notch of one grain diameter, d (typically 1μm ~ 2μm), and that the contribution of the stress intensity factor to the SiC layer by this interaction is assumed to be

$$K_I^{IPyC}\sqrt{d / a_{IPyC}}\ , \tag{38}$$

This assumption is valid because the crack tip stress field is continuous, and the stress intensity factor is proportional to the square root of the crack length. We assume a value for d of 2μm and 1μm for the IPyC and OPyC, respectively. The difference between values for these layers is because the SiC layer is deposited on the IPyC layer, and the inner surface of the SiC layer will be rougher than the outer surface.

The stress intensity factor that is induced in the SiC layer consists of two contributions, one from the PyC layer and another from the far field circumferential stress (normally compressive) in the SiC layer. Thus, the overall Mode I stress intensity factor in the SiC layer given an IPyC crack is:

$$K_I^{SiC} = K_I^{IPyC}\sqrt{d / a_{IPyC}} + \overline{\sigma}_{SiC}\sqrt{\pi d}\ . \tag{39}$$

If a OPyC crack is present, then

$$K_I^{SiC} = K_I^{OPyC}\sqrt{d / a_{OPyC}} + \overline{\sigma}_{SiC}\sqrt{\pi d}\ . \tag{40}$$

3.0 RESULTS & DISCUSSION

Figure 6 shows the results for the evolution of crack tip stress intensity factors with neutron fluence for a simulation of the stresses in one of the particles that were predicted to fail in the NPR1 irradiations using the new model. In this case the initial PyC fracture is predicted to occur at a fluence of approximately 0.8 x 10^{21} n/cm^2 in the IPyC layer. However, the resulting SiC stress intensity (remember that the net SiC circumferential stress is still compressive) is insufficient to cause SiC failure. A bit later the OPyC layer also is predicted to fail and losses its compression on the SiC layer. As a result, the stress intensity factors associated with both crack tips (one from the IPyC and the other from the OPyC) become positive. As irradiation continues, failure of the SiC is predicted to occur at a fluence of about 1.6 x 10^{21} n/cm^2.

Figure 7 shows the benchmark results for the NPR1 irradiations from both the old and the new model predictions. Table 1 shows some of the key details of the comparison. At first glance from inspection of Figure 7, it would appear that the improved model does not result in much of an improvement. However, as Table 1 shows, there are very significant improvements in the comparison in terms of the timing of the failures. Additionally, the shape of the R/B vs. time curve compares much more favorably with the actual behavior.

The one area where significant improvement is required is with the time to initial failure. We believe that one possible reason for the continuing difference between modeled and actual has to do with the re-nucleation process which must occur after PyC cracking, whereas our current assumption is that crack re-nucleation happens together with PyC cracking. Another significant factor in this is related to the possibility that partial delamination may occur in real particles during the failure process. With composite materials partial delamination may occur followed by re-initiation of the crack in the second material. Actual fuel failures are often characterized by an offset between the PyC crack and the subsequent SiC crack location. Further analysis is under way to include this type of scenario.

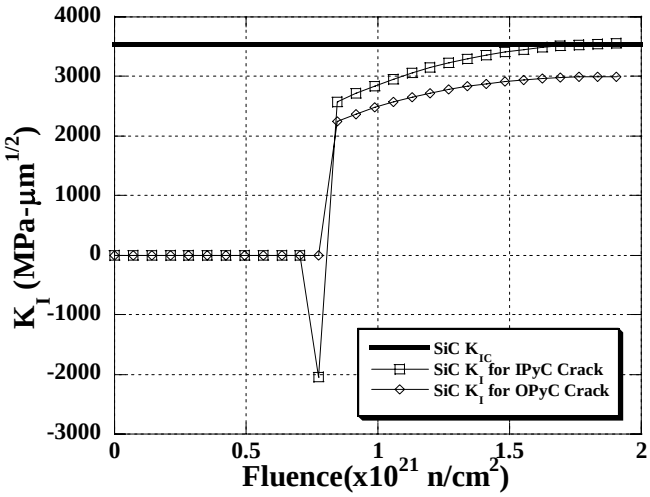

FIGURE 6 Evolution of crack tip stress intensity for IPyC and OPyC cracks as a function of fluence.

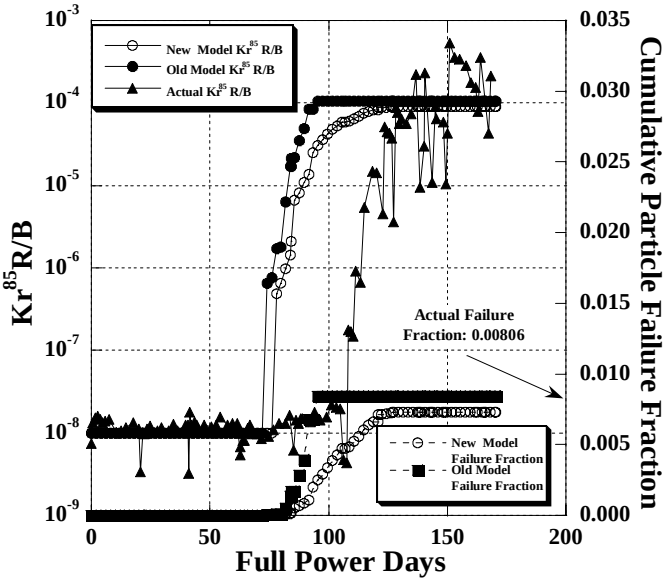

FIGURE 7 Comparison between old and improved NPR1 model calculations with observed behavior.

4.0 CONCLUSIONS

The improvements to the failure model have resulted in a more complete representation of the physics of coated particle fuel failure. These improvements have resulted in an improvement in the overall predictability of the model.

ACKNOWLEDGEMENTS

This work is sponsored by the US Nuclear Regulatory Commission (NRC).

Table 1. Comparison between results for old and improved failure models on NPR1 benchmark.

	Irradiation Test	**Original Model**	**Improved Model**
No. Particles	77500	77500	77500
No. Failed Particles	526*/625 **	656	565
Failure Probability	0.679%* 0.806%**	0.846%	0.729%
Peak Fluence at Peak Failure (10^{21}n/cm^2)	2.17	1.08	1.48
Peak Burnup at Peak Failure (% FIMA)	75.3	67.1	71.2
EFPD at Peak Failure	123.6	89.5	101.5
Peak Temperature at Peak Failure (°C)	1107	1072	1134

*Based on ionization chamber measurements
**Based on readings of the Kr^{85}m R/B

REFERENCES

1. K. Sawa, K. Minato, "An Investigation of Irradiation Performance of High Burnup HTGR Fuel", Journal of Nuclear Science & Technology 36, No. 9, 781-791 (1999)
2. G. Miller, D. Petti, D. Varacalle, J. Maki, "Consideration of the Effects on Fuel Particle Behavior from Shrinkage Cracks in the Inner Pyrocarbon Layer", Journal of Nuclear Materials, 295 (2001), 205-212, (2001)
3. J. Wang, R. G. Ballinger, and H. Maclean, "An Integrated Fuel Performance Model for Coated Particle Fuel", Submitted to Nuclear Technology
4. J. Wang. and R. G. Ballinger, "An Integrated Fuel Performance Model for the Modular Pebble Bed Reactor", ANS Winter Meeting, Reno, NV, November 2001.
5. J. Wang. and R. G. Ballinger, "A Fracture Mechanics Based Failure Model for TRISO Fuel Particles", ANS Winter Meeting, Reno, NV, November 2001.
6. J. Wang and R. G. Ballinger, "The Effect of Design and Uncertainty on Coated particle Fuel Reliability", ANS Summer Meeting, San Diego, June 1-5, 2003
7. L.A. De Lacerda and L.C. Wrobel, "Dual Boundary Element Method for Axisymmetric Crack Analysis", *International Journal of Fracture*, **113**, 267 (2002)
8. J. W. Hutchinson and Z. Suo, "Mixed Mode Cracking in Layered Materials", *Advances in Applied Mechanics*, **29**, 133 (1992)
9. H. Tada, P. Paris, and G. Irwin, "*The Stress Analysis of Cracks Handbook*", 7 & 403, ASME Press, New York (2000)